JOURNAL OF MATERIALS SCIENCE **36** (2001) 2295–2301

The effect of titanium doping on the high-temperature rhombohedral twinning of sapphire

E. SAVRUN
Sienna Technologies, Inc., 19501 144th Avenue NE, Woodinville, WA 98072, USA
E-mail: ender.savrun@siennatech.com

W. D. SCOTT
University of Washington, Seattle, WA 98105, USA

D. C. HARRIS
Code 4T42A0D, Naval Air Warfare Center, China Lake, CA 93555, USA

C-axis compressive strengths of pure and titanium-doped sapphire were measured at 600°C in air. Single crystal sapphire was doped with both titanium (3+) and titanium (4+) ions from mixtures initially containing 0.05% wt. to 0.25% wt. Ti_2O_3 in Al_2O_3. It was shown that both valence state and concentration of titanium were important in slowing down twin boundary movement under *c*-axis compression. Titanium (4+) doping did not adversely affect the thermal conductivity and infrared optical properties of sapphire.

1. Introduction

Thermal shock failure of sapphire (α-Al_2O_3) arises from rapid loss of mechanical strength at high temperatures. Loss of strength is attributed to cracking caused by intersecting rhombohedral twins [1, 2].

In the temperature range 400 to 800°C, single crystal sapphire is essentially a brittle material that does not deform by usual dislocation mechanisms. However, rhombohedral twinning is a significant mode of deformation in this temperature range, and it occurs at very low resolved shear stresses [3]. The intersection of two rhombohedral twins produces cracks that have been shown to be fracture origins for catastrophic failure [4]. The twinning process consists of two distinct stages: twin nucleation and twin growth. Twin nuclei are introduced by the machining processes and can be eliminated by polishing and annealing. Twin growth occurs by the spreading of twin boundaries, and the shear stress required for twin growth can be increased by the introduction of lattice defects which may alter the deformation mode.

The objective of this work is to demonstrate that doping sapphire with titanium (Ti^{4+}) ions can modify the twinning behavior and effectively increase the high temperature (600°C) compressive strength without adversely affecting its optical and thermal properties.

2. Titanium dopant effects on defect structure in sapphire

Defects, vacancies or dislocations can participate in the processes controlling the deformation mode and failure stress. Therefore, some background information is warranted to explain the results obtained in this study.

In sapphire the concentration of intrinsic defects is small and defect related properties of the bulk are controlled by aliovalent dopants or impurities. The process of adding a Ti^{4+} ion at an Al^{3+} site effectively adds one extra electron to the crystal. Therefore the aliovalent Ti^{4+} ion is considered to be an electron donor. Similarly, Mg^{2+} is an effective electron acceptor. It has been shown that addition of donors such as Ti^{4+} to sapphire creates aluminum vacancies V'''_{Al} [5, 6].

The oxidation-reduction reaction for sapphire in the presence of a Ti donor can be written as follows:

$$3/4\ O_2(g) + 3Ti^{x}_{Al} = 3/2\ O^{x}_{0} + 3Ti^{\bullet}_{Al} + V'''_{Al}$$

where Ti^{x}_{Al} denotes a Ti^{3+} ion on an Al^{3+} site with no effective charge; $Ti^{\bullet}_{Al}$ represents a Ti^{4+} ion substituted for an Al^{3+} ion with a positive effective charge; V'''_{Al} indicates an aluminum vacancy with a negative effective charge; and O^{x}_{0} is an oxygen ion at an oxygen lattice site. Electroneutrality requires that $3[Ti^{\bullet}_{Al}] = [V'''_{Al}]$. High oxygen pressures drive the reaction to the right, the compensated state, while low oxygen pressures (or high aluminum pressures) induce the uncompensated state; that is, the reaction goes to the left.

It has been shown that the solubility of a combination of a divalent and a tetravalent ion in sapphire is equivalent to that of a trivalent ion when straight substitution for aluminum occurs [7, 8]. The combined solubility of Mg^{2+} and Ti^{4+} in sapphire is comparable to that of Ti^{3+} and exceeds either Mg^{2+} or Ti^{4+} alone by an order of magnitude [7, 8]. It is likely that simultaneous doping of sapphire with Mg^{2+} and Ti^{4+} results in self-compensation, and the sapphire lattice exhibits

only intrinsic defect formation. This is reasonable as an overall charge balance is retained and no dopant related defect formation is required.

In general, a low concentration of dopant increases the concentration of defects of opposite charge of the type formed by disorder in the absence of dopants. For Frenkel disorder of oxygen in sapphire, these defects would be V_{Al}''' and O_i'' (aluminum vacancies and interstitial oxygen). However, owing to the larger charge of aluminum defects (V_{Al}''' and $Al_i^{\cdots}$, aluminum vacancies and interstitials), the concentration of these defects increases with dopant concentration faster than the oxygen defects because of the lower free energy of formation of the aluminum defects. Therefore, at larger dopant concentrations Al defects may become dominant.

The ionic radius of Al^{3+} is 0.53 Å. The isovalent ion Ti^{3+} (ionic radius = 0.76 Å) goes into the sapphire lattice readily during crystal growth. Incorporation of the aliovalent ions Mg^{2+} (ionic radius = 0.72 Å) or Ti^{4+} (ionic radius = 0.65 Å) creates high defect concentrations and makes crystal growth more difficult. For the present work, isovalent Ti^{3+} was selected as the dopant for investigation because it is easy to incorporate and, through various heat treatments, it could be present as a rutile (TiO_2) precipitate, an isovalent impurity (Ti^{3+}) or as an aliovalent impurity (Ti^{4+}).

3. Experimental procedure

Sapphire single crystals with and without titanium dopant were grown by the Czochralski method (Union Carbide Crystal Products, Washougal, WA). 0.050% wt., 0.10% wt. and 0.25% wt. Ti_2O_3 in Al_2O_3 were used as the dopant to provide 0.035% atomic, 0.070% atomic and 0.175% atomic Ti^{+3} concentrations in the as-grown crystals. If all of the Ti^{+3} could be converted to Ti^{+4} it would correspond to 0.055% wt., 0.11% wt., and 0.275% wt. TiO_2 concentrations. All references to weight percent in the remainder of this paper refer to the initial Ti_2O_3 in Al_2O_3.

The position of the crystal *c*-axis was determined by Laue x-ray diffraction. Four-millimeter-thick a-plane sections were sliced from the grown crystals. Compression test specimens ($3.5 \times 3.5 \times 10.0$ mm parallelepipeds) were machined in a manner that the long axis was oriented 20° off the *c*-axis towards an *r*-pole ($\bar{1}012$) on *a*-plane wafers. This configuration was chosen to enhance the shear stresses on one of the three twin planes relative to the others [9] so that one twin plane would be preferentially activated during compression testing. All surfaces of the samples were polished using a series of diamond suspensions down to 3 μm particle size. Prismatic edges of the samples were chamfered to 45° by diamond machining, and polished with 6 μm diamond suspension. The purpose of chamfering was to eliminate stress concentrations at the edges.

Pink colored, doped specimens were heated in air at 1650° C for 24 h to oxidize Ti^{3+} to Ti^{4+}, which is colorless. Undoped specimens were heat treated under similar conditions to determine the baseline strength without dopant. Heat treatments were performed in an alumina tube furnace with lanthanum chromite heating elements (Le Mont Scientific, Pittsburgh, PA). The samples were placed in high purity electronics grade alumina boats covered with alumina plates to minimize contamination of the samples during the heat treatment.

As-received and heat-treated Ti-doped samples were analyzed by electron probe microanalysis and cathodoluminescence to determine the titanium concentration and valence state to ensure a complete conversion of titanium from 3+ to 4+. The microstructure of the heat-treated sample was examined by optical and transmission electron microscopy to determine whether Ti^{4+} is in solid solution with sapphire or it exists as fine (rutile) precipitates [10].

Twin initiation stress and the ultimate compressive strength of the samples were measured by axial compression tests at 600°C in air using an Instron Model 4505 universal testing machine at a 0.5 mm/min crosshead displacement rate. Load was applied to the samples by means of alumina rams and a self-aligning alumina test fixture. Fixture surfaces in contact with the sapphire specimen were polished. Grafoil (125 μm thick corrugated graphite from UCAR Carbon Company, Cleveland, OH) was used between the sapphire and polished fixture surface as pad material throughout the study. A small vertical tube furnace was used to heat the specimens to the test temperature of 600°C in one hour without any loading. The samples were held for 10 minutes to stabilize the temperature before the testing. Temperature was monitored by a type-K thermocouple about 2 mm away from the test sample. Specimens were observed in transmitted light between crossed polarizers through *a*-surfaces and tests were recorded with a video camera for later analysis. The occurrence of twins and fracture were noted visually and the approximate stress was recorded for each event.

Indentation fracture toughness of selected samples was measured on polished a-plane surfaces in two different orientations, as shown in Fig. 1. In orientation (A) microcracks would form on primary ($01\bar{1}2$) and secondary ($\bar{1}012$) twin planes, parallel to indent diagonals. In orientation (B) microcracks are expected to form on the basal plane (0001) and the m-plane ($10\bar{1}0$). By choosing orientation A, we attempted to simulate mode I crack opening on the primary twin plane ($01\bar{1}2$)

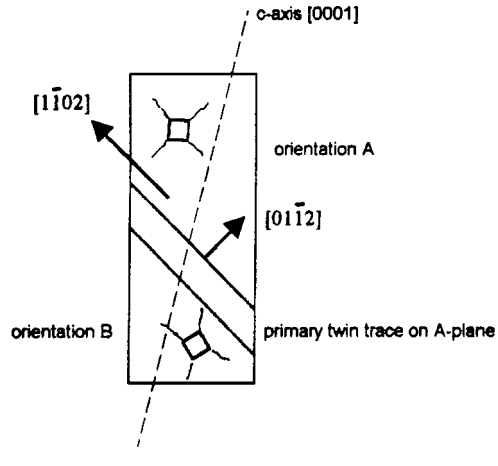

Figure 1 Indent orientations on *a*-plane (see text for descriptions).

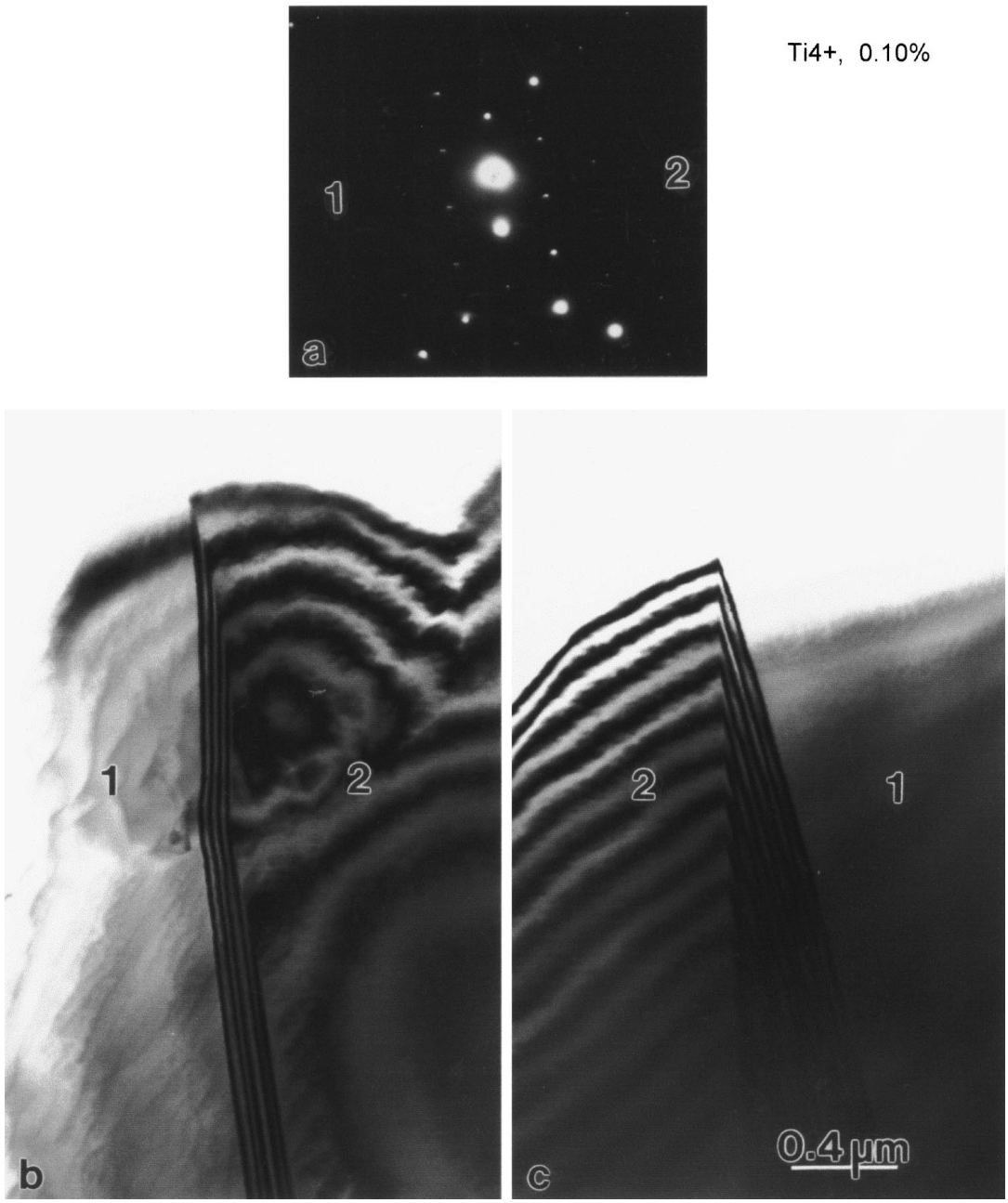

Figure 2 Transmission electron micrograph of a twin boundary in a Ti^{4+} doped sample from 0.10% wt. Ti_2O_3. The Selected Area Diffraction pattern (upper image) shows that we are looking at the twin boundary.

and thus observe any effect Ti^{4+} doping may have on the primary and secondary twin planes. The purpose of choosing orientation B was to introduce microcracking on the basal plane so that the effect of Ti^{4+} doping could be studied.

A load of 9.8 N for 15 s was used for each indentation using a Vickers diamond indenter. At least 5 measurements were made for each orientation for each sample. Microcrack and twin lengths formed around the indent were measured right after indentation using 500× magnification in an optical microscope. Rapid analysis of the damage around the indent was necessary, because it was shown that the extent of damage could change as function of time once the indent formed [11, 12]. Fracture toughness was calculated by the method of Antis *et al*. [13] for microcracks in orientation A. Fracture toughness was not calculated for orientation B because no stable crack formation occurred starting from the indent corners. In fracture toughness calculations, 425 GPa and 336 GPa were taken as the elastic modulus of both doped and undoped samples in orientation A for primary and secondary twin planes, respectively [14].

Infrared transmission and optical scatter were measured on a 0.10% wt. Ti_2O_3-doped sample (1.5 mm thick) before and after heat treatment. Transmission was measured on *c*-plane disks using a Nicolet 710 FTIR spectrophotometer at a resolution of 4 cm^{-1}. Total integrated scatter was measured by the method of Archibald and Bennett [15]. Infrared emittance was measured at the Johns Hopkins University Applied Physics Laboratory with an emissometer described previously [16]. Sapphire was heated from the back surface

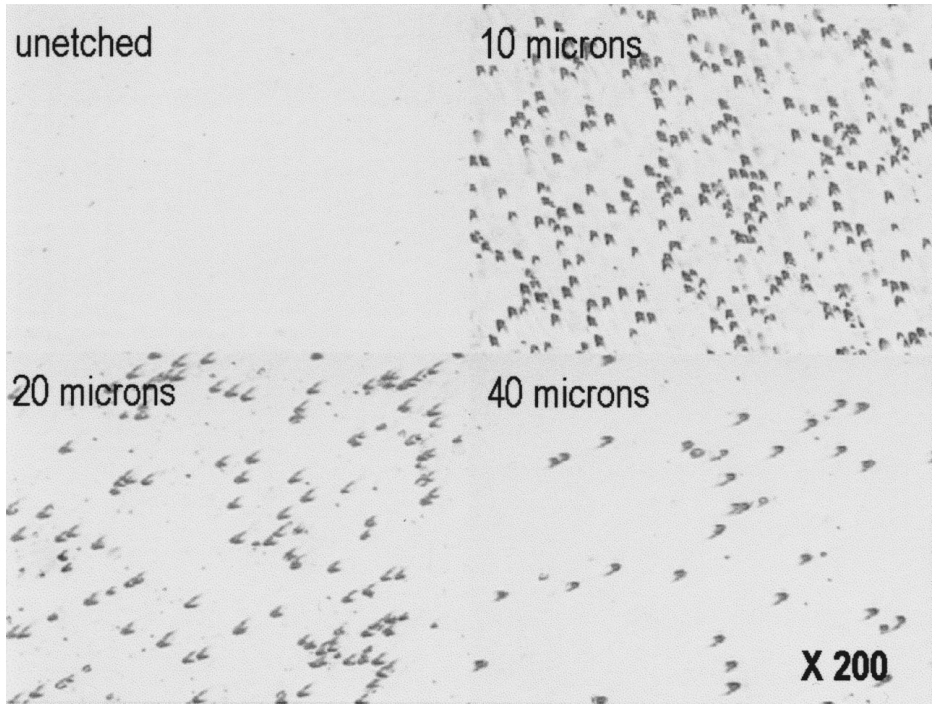

Figure 3 Etch pits on *a*-plane of Ti^{4+}-doped sapphire from 0.25% wt. Ti_2O_3 as a function of surface depth. Material is removed by borax etching.

by a CO_2 laser at 10.6 μm while emission from the front surface was measured with a Bomen DA3 interferometer. The spectrum of the ambient temperature background was subtracted from the observed spectrum. Emission from sapphire was compared to that of a blackbody at the same temperature. Thermal conductivity was measured on *c*-plane disks using the laser flash method. Back and front surfaces of the samples were coated with gold and carbon to absorb laser light. A laser beam was shined on the front surface of the disks and temperature rise was measured on the back surface. From the half-rise time, thermal diffusivity and thermal conductivity were calculated.

4. Results and discussion

4.1. Microstructural characterization

Electron probe microanalysis of the 0.10% wt. Ti_2O_3-doped (heat treated at 1650°C for 24 h in air) specimens showed that the equivalent TiO_2 concentration was 0.16% wt. rather than the expected 0.11% wt. TiO_2 at the edge of a compression specimen. However, microprobe analysis of the center of the same compression specimen showed that the equivalent TiO_2 concentration was 0.09% wt. The titanium concentration of the second doped composition (0.25% wt. Ti_2O_3) was between 0.20 and 0.25% wt. Ti_2O_3 in the crystal. The cathodoluminescence color of an as-doped sample was intense red—characteristic of Ti^{+3}. The cathodoluminescence color of heat-treated sample was pale bluish white—characteristic of Ti^{+4}. These colors suggest that all Ti^{+3} was converted into Ti^{+4} upon heat treatment.

No precipitates could be detected under the transmitted light microscope (up to 1000×) after heat treatment of any Ti doped samples. The transmission electron micrographs in Fig. 2 show matrix (1), twinned region (2), and the matrix/twin boundary of 0.10% wt. doped sapphire. Fig. 2b and c show that the twin boundary is free of precipitates and defects. This finding suggests that Ti^{4+} enters the sapphire lattice most likely as a substitutional ion on aluminum sites.

TABLE I Compressive strength of sapphire as a function of Ti dopant concentration and surface polishing technique

Sample	No. of Samples	σ_{twin}, (MPa)*	σ_{max}, (MPa)*	σ_{max} Range (MPa)
Undoped Sapphire				
Mechanical Polish	7	128 ± 18	162 ± 17	135–180
Mechanical Polish + Heat treatment at 1650°C for 24 hours	4	326 ± 57	398 ± 25	361–413
0.25% Ti_2O_3-doped				
Ti^{3+}, Mechanical Polish	2	118	142	101–183
0.050% Ti_2O_3-doped				
Ti^{4+}, Mechanical Polish	3	245 ± 18	374 ± 54	327–434
Ti^{4+}, Mechanical Polish + Borax etch	2	300	424	342–507
0.10% Ti_2O_3-doped				
Ti^{4+}, Mechanical Polish	7	332 ± 38	437 ± 66	332–542
Ti^{4+}, Mechanical Polish + Borax etch	2	235	330	289–372
0.25% Ti_2O_3-doped				
Ti^{4+}, Mechanical Polish	11	331 ± 61	441 ± 57	360–451
Ti^{4+}, Mechanical Polish + Borax etch	3	Not observed	615 ± 29	597–649
Ti^{4+}, Mechanical Polish + controlled scratch	3	297 ± 46	424 ± 64	357–485

*Mean ± standard deviation.

4.2. Compressive strength

Compressive strengths are listed in Table I. σ_{twin} is the stress at which the first twin was observed. σ_{max}

TABLE II The effect of titanium doping on twin growth

Sample	Twin width, μm
Undoped, as-polished	175
Ti^{4+} from 0.10% wt. Ti_2O_3 doping	31
Ti^{4+} from 0.25% wt. Ti_2O_3 doping	18
Ti^{3+} from 0.25% wt. Ti_2O_3 doping	40

is the maximum stress in the specimen before it failed. σ_{max} is considered to be the compressive strength of the specimen.

There is no significant difference in twin initiation stress or compressive strength of undoped and Ti^{3+} doped as-polished samples in Table I. When doped material is annealed at 1650°C to convert Ti^{3+} to Ti^{4+}, σ_{twin} and σ_{max} both increase significantly. However, if undoped sapphire is annealed under the same conditions, σ_{twin} and σ_{max} increase also. Ti^{4+} doped sapphire does not have significantly higher strength than undoped sapphire subjected to the same annealing.

The most significant effect of Ti doping was, however, to slow down the twin propagation rate significantly over the undoped samples, as observed by video imaging recorded under polarized light, and as illustrated by the twin widths listed in Table II. Undoped samples failed within 12–15 s from the start of testing while Ti^{4+}-doped samples failed 30 s or more after the test started. In obtaining the twin width data in Table II, samples were loaded just above the twin initiation stress and then the tests were stopped and twin widths were measured under polarized light with a light microscope. Twin width decreased with increasing Ti^{4+} dopant concentration. Furthermore, when the sides of Ti^{4+}-doped samples are ground (260 grit fixed abrasive diamond) to introduce controlled surface flaws for twin initiation, the compressive strength did not change significantly for 0.25% wt. Ti_2O_3-doped samples, as shown by the last entry in Table I. These observations and the data in Table II clearly suggest that titanium doping significantly reduces the twin propagation rate.

Ti^{3+}-doped (0.25% wt.) and undoped samples showed similar strengths, 142 MPa and 162 MPa, respectively. Upon oxidation of Ti^{3+} to Ti^{4+}, it is likely that as Ti^{4+} ion replaces Al^{3+} in the crystal, aluminum vacancies form to maintain the charge balance [5, 6]. The position of vacancies in the crystal structure is not known, but it is possible that they may create stacking faults on the twin planes, thus making twin propagation more difficult.

Table II shows that as the Ti^{4+} concentration increases, the twin width decreases. This is consistent with the observation during 600°C compression testing that fewer twins form and they tend to run slower in the Ti^{4+} doped samples. That is, the twins widen and move forward from the edge into the specimen more slowly when Ti^{4+} is present. In Ti^{3+}-doped samples, even though twin widths are relatively narrow, many more twins form and tend to grow together, which accounts for the lower strength (142 MPa) of Ti^{3+}-doped samples.

Ionic size mismatch alone is not responsible for the observed strengthening effect, if one recalls that the ionic size of Al^{3+} is 0.53 Å, Ti^{3+} is 0.76 Å, and Ti^{4+} is 0.65 Å in six-fold coordination. Ti^{3+} is larger than Ti^{4+}, but Ti^{4+} exerts a greater effect in retarding twin propagation.

To reduce the effects of machining damage in Ti^{4+} doped samples, a borax etching method was developed. Samples were exposed to molten borax at 910°C for 2 min per cycle. As estimated from mass loss, each cycle removed 10 microns of material from the sample surfaces. Optical microscope images taken from the etched surfaces of 0.25% wt. Ti_2O_3-doped sample revealed that the extent of machining damage could be as deep as 40 μm as illustrated in Fig. 3. As the number of etch pits decreases in Fig. 3, the number of defects decreases.

The greatest strength increase was achieved when the mechanically polished surfaces of 0.25% wt. Ti-doped samples were chemically polished using molten borax. In these samples twin initiation stress could not be recorded since no twins were observed prior to mechanical failure. Samples failed in a typical brittle manner, with an average compressive strength of 615 ± 29 MPa.

These results suggest that Ti^{4+} doping combined with removal of machining damage from the surface can increase the maximum compressive strength of sapphire. Twin initiation can be avoided by eliminating gross machining defects, which cause premature failures.

4.3. Indentation fracture toughness

Room temperature micro-indentation tests were carried out on a-planes of undoped, Ti^{3+} 0.25% wt., Ti^{4+} 0.25% wt., and Ti^{4+} 0.11% wt doped sapphire. Fracture toughness values on primary $(01\bar{1}2)$ and secondary $(\bar{1}012)$ twin planes are shown in Table III. The average fracture toughness values on the secondary twin planes

TABLE III Indentation fracture toughness of sapphire on primary $(01\bar{1}2)$ and secondary $(\bar{1}012)$ twin planes

	K_{IC} (MPa · $m^{1/2}$)		Basal Twin Length (microns)
Sample	$(01\bar{1}2)$	$(\bar{1}012)$	*a*-plane
Undoped	1.87 (±0.13)	1.40 (±0.14)	261
Undoped heat treated at 1650 °C, 24 hrs.	1.50 (±0.17)	1.37 (±0.34)	171
Ti^{3+} from 0.25% wt. Ti_2O_3	1.93 (±0.24)	1.66 (±0.19)	73
Ti^{4+} from 0.25% wt. Ti_2O_3	1.96 (±0.29)	1.76 (±0.32)	25
Ti^{4+} from 0.10% wt. Ti_2O_3	1.98 (±0.23)	1.58 (±0.25)	23

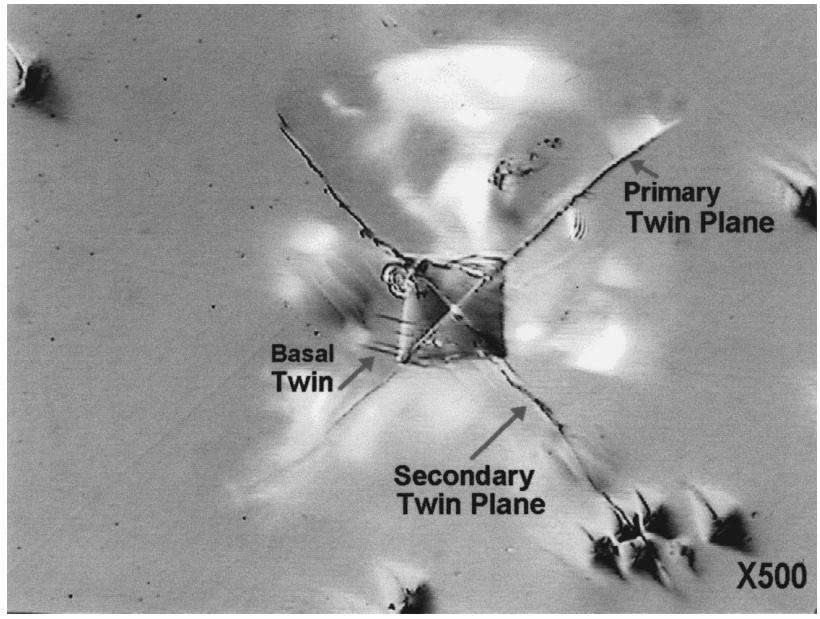

(a)

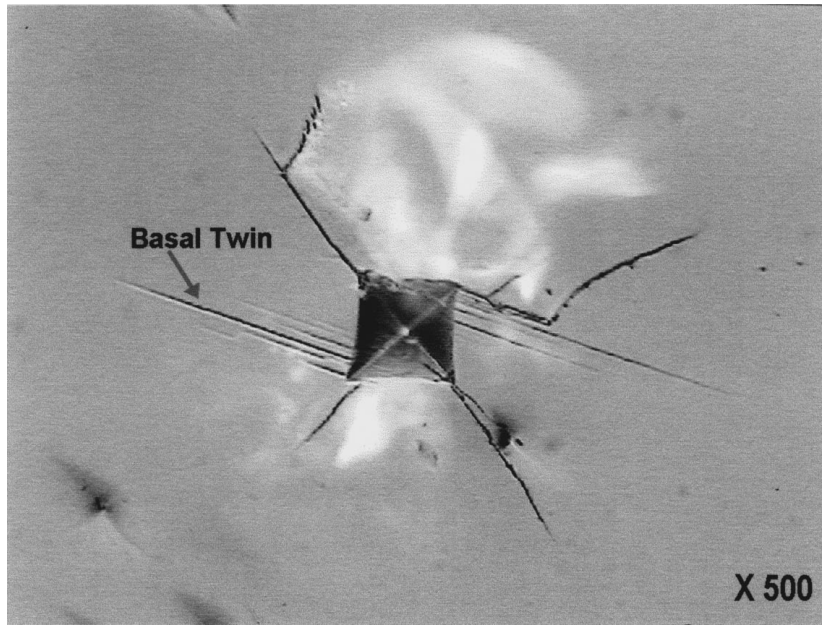

(b)

Figure 4 Basal twins and indentation micro cracks formed on the *a*-plane around the indents of Ti^{4+}-doped sapphire from 0.10% wt. Ti_2O_3. (a) Doped and (b) Undoped sapphire surfaces. Arrow indicates primary twin trace.

are slightly less than what is measured on primary twin planes for all the samples, but the differences are within the standard deviations. Overall, fracture toughness values are lower than what is reported in the literature [12, 17]. Iwasa and Bradt [17] measured the room temperature fracture toughness of undoped sapphire as 2.38 and 2.43 after introducing a controlled micro-cracks on *r*- and *a*-planes of a flexure test sample, respectively. Smith and Pletka [12] reported the fracture toughness of 0.05% wt. Ti^{4+} and Ti^{3+} samples as 2.61 and 2.66, respectively, using micro-indentation on basal planes of sapphire with Vickers indenter diagonals aligned parallel to *a*- and *m*-planes. The present results are significantly lower than those of Pletka, because significant amounts of basal twinning occurred, especially in undoped and Ti^{3+}-doped samples, as shown in Fig. 4 and Table III. This means that some of the energy was used for basal twin formation instead of crack propagation on twin planes. Therefore, fracture toughness values of undoped and Ti^{3+}-doped samples are likely to be overestimated. The fracture toughness of Ti^{4+}-doped sapphire is therefore greater than the toughness of undoped or Ti^{3+}-doped material, for crack propagation on the *r*-planes.

4.4. Optical and thermal properties

Infrared transmission and optical scatter of undoped and doped samples before and after heat treatment are shown in Table IV. The scatter at 3.39 μm in all samples is quite low and in a reasonable range for an infrared optical window. The transmission data also suggest that titanium doping and subsequent heat treatment have little effect on infrared transmission. Fig. 5 compares

TABLE IV Infrared total integrated scatter and infrared transmission at 3.39 μm in undoped, Ti^{3+}, and Ti^{4+} doped sapphire. (1.5 mm thick *c*-plane disks)

Sample	Scatter at 3.39 μm*	Transmission at 3.39 μm, %
Undoped	$0.28 \pm 0.05\%$	87.1
Ti^{3+} from 0.10% wt. Ti_2O_3	$0.35 \pm 0.10\%$	86.5
Ti^{4+} from 0.10% wt. Ti_2O_3	$0.35 \pm 0.07\%$	85.8
Ti^{4+} from 0.25% wt. Ti_2O_3	—	85.0

*Total integrated scatter in forward hemisphere measured between 2.5° and 70° from specular direction.

TABLE V Thermal conductivity of undoped and Ti-doped sapphire

Sample	Thermal conductivity W/m·K 25°C	300°C	600°C
Undoped	37.1	15.4	10.3
Ti^{4+} from 0.10% wt. Ti_2O_3	36.8	14.6	10.0
Ti^{4+} from 0.25% wt. Ti_2O_3	37.1	15.5	10.6

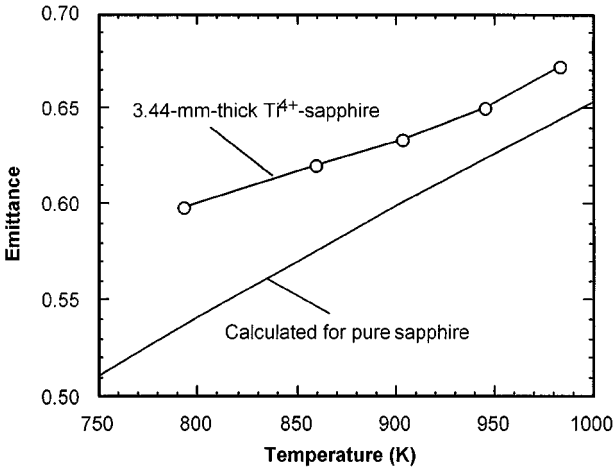

Figure 5 Emittance at a wavelength of 5 μm from Ti^{4+}-doped *c*-plane sapphire prepared from 0.25% wt. Ti_2O_3 that was heated to 1650°C in air for 48 h to produce a very pale pink disk with a thickness of 3.44 mm. For comparison, the emittance of 3.44-mm-thick *c*-plane sapphire computed with absorption coefficients and refractive index from the program OPTIMATR® [18] is shown.

the measured emittance of Ti^{4+}-doped sapphire at a wavelength of 5 μm with the emittance expected for pure sapphire of the same thickness. The two curves are generally within 10% of each other.

Thermal conductivities of both undoped and doped sapphire in Table V decrease with increasing temperature. However, Ti^{4+} doping does not degrade the thermal conductivity of sapphire between room temperature and 600°C.

5. Conclusions

- Heat treatment of Ti^{3+} doped and undoped sapphire more than doubles the *c*-axis compressive strength of sapphire at 600 °C.
- Doping the sapphire crystal with Ti^{4+} ions does not further increase strength, but slows twin boundary movement during rhombohedral twinning at 600°C. Twin width decreases with increasing Ti^{4+} concentration.
- Elimination of surface/subsurface machining damage by chemical polishing is very effective in raising the twin initiation stress and the compressive strength of sapphire. A combination of Ti^{4+} doping and surface treatment increased the compressive strength of 0.25% wt. Ti_2O_3 doped sapphire to 615 MPa without any observable twin formation.
- Titanium doping and subsequent heat treatment have little effect on the infrared transmission, emission, and optical scatter of sapphire.
- Titanium doping does not affect the thermal conductivity of sapphire up to 600°C.

Acknowledgments

This work was sponsored by the Office of Naval Research. We thank Prof. Mehmet Sarikaya of University of Washington for transmission electron microscopy work, Dr. Cetin Toy for compression testing and fracture toughness measurements, and Dr. Bruce Cook of Iowa State University for thermal conductivity measurements. Emittance was measured by M. E. Thomas, M. J. Linevsky and J. W. Giles at the Johns Hopkins University Applied Physics Laboratory, Laurel, MD. Infrared transmission and scatter were measured by Mel Nadler and Joni Pentony at the Naval Air Warfare Center.

References

1. D. C. HARRIS, F. SCHMID, J. J. MECHOLSKY, JR. and Y. L. TSAI, in *Proceedings of SPIE* **2286** (1994) 16.
2. F. SCHMID and D. C. HARRIS, *J. Amer. Ceram. Soc.* **81** (1998) 885.
3. W. D. SCOTT and K. K. ORR, *ibid.* **66** (1983) 27.
4. R. L. BERTOLOTTI and W. D. SCOTT, *ibid.* **54** (1971) 286.
5. S. K. MOHAPATRA and F. A. KROGER, *ibid.* **60** (1977) 381.
6. R. T. COX, *J. de Physique* **34** (1973) C9-333.
7. T. P. JONES, R. L. COBLE and C. J. MOGAB, *J. Amer. Ceram. Soc.* **5** (1969) 331.
8. G. A. KEIG, *J. Cryst. Growth* **2** (1968) 356.
9. F. G. KARP, M.Sc. Thesis, University of Washington, Seattle, 1984.
10. R. J. BRATTON, *J. Appl. Phys.* **42**(1) (1971) 211.
11. B. MULLER, *Cryst. Res. and Tech.* **19**(8) (1984) 1113.
12. S. S. SMITH and B. J. PLETKA, in "Fracture Mechanics of Ceramics," Vol. 6, edited by R. C. Bradt *et al.* (Plenum, New York, 1983) p. 189.
13. G. R. ANTIS, P. CHANTIKUL, B. R. LAWN and D. B. MARSHALL, *J. Amer. Ceram. Soc.* **64** (1981) 533.
14. M. KAJI, Ph.D. Thesis, University of Washington, Seattle, 1988.
15. P. C. ARCHIBALD and H. E. BENNETT, *Opt. Eng.* **17** (1978) 647.
16. M. J. LINEVSKY, R. M. SOVA, M. E. THOMAS, R. I. JOSEPH and F. F. MARK, *Johns Hopkins APL Technical Digest* **13**(3) (1992) 368.
17. M. IWASA and R. C. BRADT, in "Structure and Properties of MgO and Al_2O_3 Ceramics" (The American Ceramic Society, 1984) p. 767.
18. OPTIMATR® (ARSoftware, Landover, MD). A Computer Program to Calculate Optical Properties of Materials.

Received 10 February
and accepted 31 July 2000